remote sensing

MDPI

Article

Incorporating Density in Spatiotemporal Land Use/Cover Change Patterns: The Case of Attica, Greece

Dimitrios Gounaridis [1,*], Elias Symeonakis [2], Ioannis Chorianopoulos [1] and Sotirios Koukoulas [1]

[1] Department of Geography, University of the Aegean, 81100 Mytilene, Greece; I.Chorianopoulos@geo.aegean.gr (I.C.); skouk@geo.aegean.gr (S.K.)
[2] School of Science and the Environment, Manchester Metropolitan University, Manchester M1 5GD, UK; e.symeonakis@mmu.ac.uk
* Correspondence: gounaridis.d@geo.aegean.gr; Tel.: +30-22510-36427

Received: 12 June 2018; Accepted: 29 June 2018; Published: 1 July 2018

Abstract: This paper looks at the periodic land use/cover (LUC) changes that occurred in Attica, Greece from 1991 to 2016. During this period, land transformations were mostly related to the artificial LUC categories; therefore, the aim was to map LUC with a high thematic resolution aimed at these specific categories, according to their density and continuity. The classification was implemented using the Random Forests (RF) machine learning algorithm and the presented methodological framework involved a high degree of automation. The results revealed that the majority of the expansion of the built-up areas took place at the expense of agricultural land. Moreover, mapping and quantifying the LUC changes revealed three uneven phases of development, which reflect the socioeconomic circumstances of each period. The discontinuous low-density urban fabric started to increase rapidly around 2003, reaching 7% (from 2.5% in 1991), and this trend continued, reaching 12% in 2016. The continuous as well as the discontinuous dense urban fabric, almost doubled throughout the study period. Agricultural areas were dramatically reduced to almost half of what they were in 1991, while forests, scrubs, and other natural areas remained relatively stable, decreasing only by 3% in 25 years.

Keywords: land use/cover; change detection; Random Forests; semi-automated classification; thematic resolution

1. Introduction

Research efforts related to land use/cover (LUC) change have intensified since the mid-1970s, with the realization that processes taking place on the Earth's surface directly and indirectly affect the climate and the environment [1]. An important distinction between the concepts of land use and land cover is the fact that the former focuses on economic activities occurring on a given surface of the land, while the latter refers to the physical attributes of the Earth's surface [2]. Given that the alteration of the Earth's surface by human activity is substantial and ever growing, any significant changes in land use affect land cover and vice versa [3]. Through a complex mechanism, pertaining to complex theory, changes in land cover affect land use locally, while also contributing to wider-scale processes such as climate change [4], desertification [5], and global environmental change [6]. Moreover, land cover changes hold wide-ranging significance for the structure and function of ecosystems, with equally far-reaching consequences for humans in every aspect.

Field data approaches for assessing LUC change face several limitations as they are resource-demanding in terms of personnel, equipment, and time, they are limited by topographic and

climatic conditions and low accessibility to remote areas and are therefore restricted to the local scale. Earth Observation (EO) technologies, along with Geographic Information Systems (GIS), can be combined to successfully provide spatially consistent and detailed LUC information, a prerequisite for monitoring the Earth's surface effectively [7,8]. To this end, the recent increase in the available EO data [9] can facilitate the growing demand for multi-spectral and multi-temporal information over a wide range of scales and data formats (e.g., [10–12]). However, adopting EO techniques and relying on satellite data involves facing a trade-off between spatial scale and cost: very high resolution (VHR) imagery are expensive (e.g., Worldview, IKONOS), which acts as an obstacle to carrying out large-scale and multi-temporal approaches. Low resolution data (e.g., AVHRR, MODIS), on the other hand, are free of charge and in abundance. However, this type of data may be unsuitable for monitoring certain processes and for capturing patterns that usually occur on a finer scale, such as LUC changes.

With the Landsat program running for more than four decades now, medium spatial resolution satellite images have been widely used for monitoring LUC and associated changes [13]. The advantages of using Landsat data are the suitable spatial resolution of 30 m for LUC monitoring, the high temporal resolution due to the low revisit cycle of the satellite and the spectral resolution offered. To add to that, the opening of the Landsat archive in 2008, offering readily available data at no cost, makes it the only feasible option for studies that span decades and cover large extents [14].

Recent technological and methodological advancements have contributed to the availability of LUC datasets at various resolutions. However, their limitations and challenges related to their nomenclature, their accuracy, and their interoperability still remain to be addressed [15,16]. Often, the use of readily available datasets in a range of research applications and land management decision-making is limited by their low thematic resolution, that is, the detail in the definition of LUC categories. Thematic resolution directly determines the amount of detail of geospatial information contained in categorical data produced from 'hard' classification, which in turn defines how meaningful and useful a map can be for providing answers to a range of research questions. Several studies have stressed the importance of thematic resolution in different applications, for example in land use modeling [17,18], land-cover pattern analysis [19], species distribution modeling [20], land surface temperature modeling [21], and landscape indices behavior [22,23]. However, although thematic resolution is acknowledged as an important property, in most cases available datasets represent important LUC categories lumped into one or two broad classes, which is rarely the case on the ground [24]. Therefore, the uptake of these datasets by research efforts focusing on areas that face a multitude of LUC transformations is limited. Depending on the study area and the dominant LUC transformations, the discrimination of LUC categories according to their density and continuity is crucial. For example, in areas that have undergone different types of urbanization, in terms of changes that have occurred in the extent but also in the density of the urban fabric, such discrimination can reveal important insights. The same applies to research efforts focusing on LUC transformations in forested areas and/or cropland.

To avoid these limitations, studies that aim to assess LUC changes occurring in a specific area and period of time cannot often rely on existing 'hard' classified datasets, such as the CORINE [25] or the GLOBELAND 30 [26]. Temporally consistent and accurate LUC maps need to be produced to satisfy the growing demand for spatially explicit and accurate LUC data. To this aim, several research efforts have focused on introducing increasingly sophisticated approaches, which, at the same time, are less resource-demanding and labor-intensive. A clear trend can be identified in the development of automated (e.g., [27–31]) or semi-automated (e.g., [32–34]) LUC classification approaches. A common and important element of these approaches for accomplishing a minimum use intervention is the utilization of existing and readily available LUC data for training the classifier. Under the assumption that changes usually occur only to a small fraction of the land, incorporating accurate but relatively outdated information in the classification process is a reasonable and promising pathway to follow in order to eliminate the remaining gaps in the LUC mapping literature [27,30,32–35].

Our main aim in this paper is, therefore, to explore the spatiotemporal LUC patterns in the Attica region of Greece, spanning 25 years, that have seen changes originating from different socioeconomic realities. Due to the fact that the area has been subjected to significant artificial land transformations, our specific objectives include the mapping of a high thematic resolution in these categories, discriminating the urban category according to its density and continuity. Change detection techniques in the form of cross-classification and cross-tabulation are also applied to map and quantify the periodic LUC changes. The former allows the mapping of changes, while the latter allows their tabulation. Our approach is able to shed light on the different economic performance realities and land-use planning contexts and choices that Attica faced during the study period. It is also fully transferable to other regions, contains a high degree of automation, and can act as a baseline for the continuous monitoring of LUC using medium-scale EO data.

2. Materials and Methods

2.1. Study Area

The study area is the region of Attica in mainland Greece (total area approximately 3000 km^2), the focal point of the rapid socioeconomic transformations that occurred in the country during the last decades. The region includes the City of Athens—the capital of Greece—and adjacent municipalities, forming the Athens conurbation, which is inhabited by approximately 4 million people or ~35% of the total population of Greece. Athens attracted the majority of its population in the postwar years, as part of a major urbanization wave underscored by a persistent increase in housing demand and supply [36]. Since the early 1980s, however, economic growth triggered the residential decentralization of middle-class strata, seeking a better quality of life in areas outside the Athenian conurbation, within a reasonable commuting distance from their jobs [37]. Residential mobility, however, remained confined within the region and took the form of amenity homes ('exochikó') located primarily along the seacoast [38]. As a consequence, the landscape of the Athenian urban periphery changed substantially over the years. Urban growth, however, was particularly unregulated, marked by the absence of land use planning checks and controls [39]. The establishment of the regional Master Plan as early as 1985 did not change trends on the ground. Its implementation was postponed and its guidelines were persistently ignored [40]. Instead, development was permitted despite any medium- or long-term negative externalities and environmental costs. Moreover, after successfully attracting national and foreign funds and in the face of hosting the Olympic games of 2004, the demand for construction sites to accommodate commercial, industrial, transportation, and recreational activities further increased the built-up transformation of the urban periphery [41]. However, after a relatively stable period of successive economic growth, the area has recently been exposed to the negative consequences of the global financial crisis (2008), succeeded by the sovereign debt crisis (2010) and a prolonged economic recession [42]. Negative growth rates and economic contraction hampered the housing and construction industries [43]. In the 2010–2014 period, for instance, the number of transactions in the real estate market in the region fell by approximately 78% [44]. Athens also constitutes an interesting study case due to its undulated morphology (Figure 1). The geomorphological features of the region dictate the land availability and determine the accessibility and the optimal conditions for urban construction. The plain of the city of Athens is surrounded by mountains (Egaleo, Parnitha, Penteli, and Hymettus), with elevations ranging from 1 m to 1350 m. These morphological features separate Athens from the other relatively flat districts of Thriasio, Messoghia, and Marathonas, which, together with Athens, make up the only available areas in Attica to host urban construction.

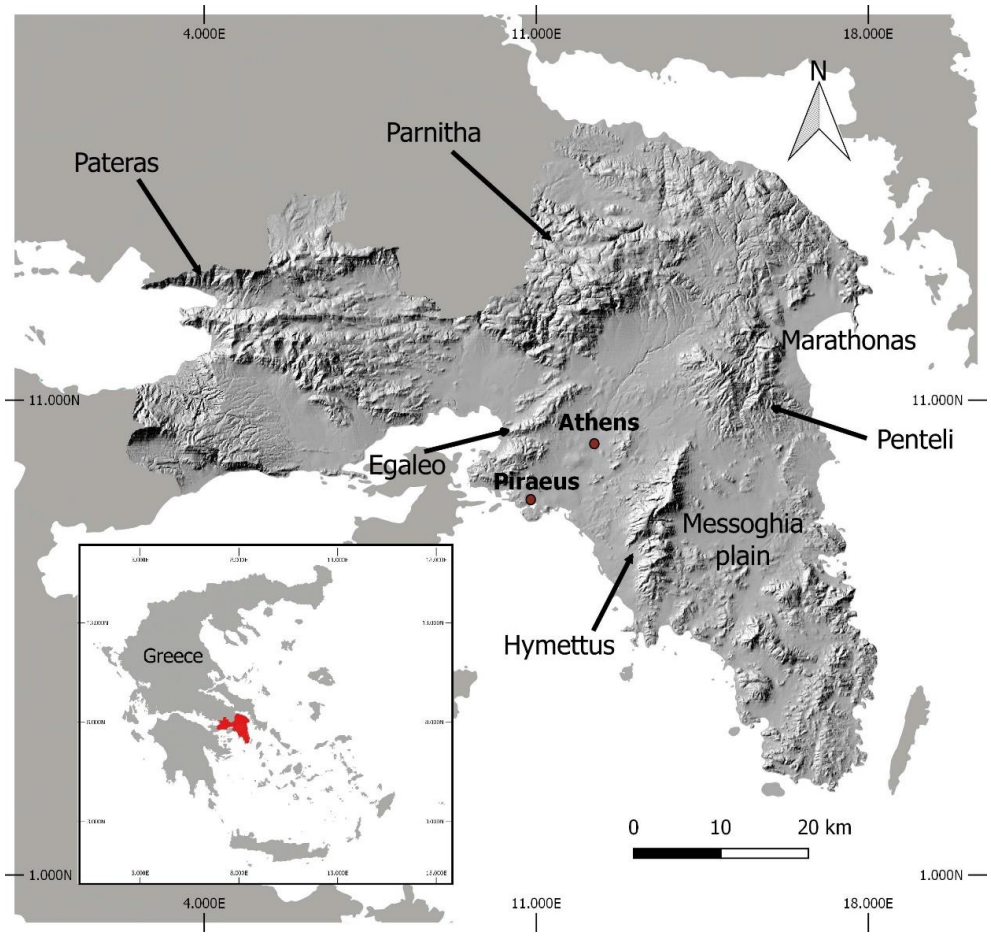

Figure 1. Location and topography of the Attica region.

2.2. Data Used

Since the Attica region is fully covered by two consecutive images (path: 183, row: 033–034), a total of 10 Landsat images (Table 1) spanning 25 years (1991–2016) were chosen to achieve full geographical coverage. The acquired images meet certain quality standards, namely, no cloudiness in the study area, acquisition during summer months to avoid phenological variations, and the absence of the scan line corrector problem of Landsat 7 after 2003.

Table 1. The characteristics of the satellite images used as the primary data to perform the change detection analysis.

Date	Sensor	Satellite	Resolution (m)	Path/Row
17 September 1991	Thematic Mapper (TM)	Landsat 4	30	183/034
29 June 1991	Thematic Mapper (TM)	Landsat 4	30	183/033
22 August 1999	Enhanced Thematic Mapper Plus (ETM+)	Landsat 7	30	183/034
22 August 1999	Enhanced Thematic Mapper Plus (ETM+)	Landsat 7	30	183/033
12 October 2003	Thematic Mapper (TM)	Landsat 5	30	183/034
12 October 2003	Thematic Mapper (TM)	Landsat 5	30	183/033
12 August 2010	Thematic Mapper (TM)	Landsat 5	30	183/034
12 August 2010	Thematic Mapper (TM)	Landsat 5	30	183/033
29 September 2016	Operational Land Imager (OLI)	Landsat 8	30	183/034
29 September 2016	Operational Land Imager (OLI)	Landsat 8	30	183/033

2.3. Image Pre-Processing

To avoid any discrepancies due to the multi-temporal and multi-sensor type of analysis and to efficiently compute spectral indices, all images underwent radiometric as well as atmospheric correction. To do so, the initial digital numbers (DN) were converted to top of atmosphere reflectance using the dark-object subtraction method introduced by Chavez [45]. Then, surface reflectance values were calculated by applying the 6S model [46]. Topographic normalization was also important in order to minimize the topographical effects due to the mountainous nature of the terrain. After computing the illumination angle [47], we applied the C-correction method originally developed by Teillet et al. [48]. Next, the two consecutive calibrated images per year were mosaiced, resulting in five images spanning 25 years (1991, 1999, 2003, 2010, 2016).

2.4. Sampling and Validation

The choice of LUC categories was dictated by our objective to obtain LUC information with a high thematic resolution, especially for the urban types because this LUC category is dominant and exhibited the most pronounced changes in our study area. We opted to follow the classification system adopted by the Urban Atlas [49] database, as it classifies the urban category into five classes differentiated by the degree of imperviousness. This degree is defined by the total fraction of land covered by pavement structures that are covered by impenetrable materials. Therefore, following this nomenclature for our case, the chosen LUC categories were: (i) continuous urban fabric (degree of imperviousness >80%); (ii) discontinuous dense urban fabric (degree of imperviousness 50–80%); (iii) discontinuous medium density urban fabric (degree of imperviousness 30–50%); (iv) discontinuous low density urban fabric (degree of imperviousness 0–30%); (v) industrial, commercial, and transport units; (vi) arable land and permanent crops; (vii) forests, scrubs, and other natural areas; and (viii) other, which included open spaces bare, mines, and inland water bodies.

The LUC categories were distinguished by devising a semi-automated sampling extraction based on a context that combined the no-change areas, prior knowledge, and spectral controlling. More specifically, starting with 2010 and 2016, an extensive sampling was designed based on the visual interpretation of very high spatial resolution data from Google Earth and on existing available reference LUC data. In particular, two LUC datasets at the national scale and 30 m resolution were used as reference data for the semi-automated sampling extraction. The first classifies the urban category into five sub-categories according to density and continuity and in accordance with the classification system of Urban Atlas [50], and the second classifies Greece into 12 broader categories of LUC [32]. For the non-artificial LUC types of croplands, forest, scrubs, other natural areas, and other, additional samples from the Urban Atlas and CORINE datasets [25,49] were also assembled to strengthen the training. A quality control mechanism to remove outliers from the analysis, based on the spectral signatures of the samples, was also applied—excluding from the analysis all outliers per class [30]. For the 1991, 1999, and 2003 images, a backwards automated training strategy was adopted. Given the fact that other high-resolution reference data for these dates do not exist, and that changes usually occur on a fraction of the total area, the use of the unchanged areas as training samples for the past dates is reasonable [27,51]. No-change areas were identified via the visual interpretation of very high spatial resolution data from Google Earth. These no-change areas were then used to semi-automatically generate training samples as input for the subsequent classification of each year. Special attention was paid to avoid taking points close to the boundaries of adjacent LUC categories, ensuring that clear samples of each category were taken and thus eliminating any source of confusion in the model [32]. Seventy percent of the samples were used to train the RF algorithm, while the remaining 30% were kept for the accuracy assessment of the results (Table 2).

Table 2. Training and validation samples used for classification modeling.

LUC Categories	Training				
	1991	1999	2003	2010	2016
Continuous urban fabric	1798	2321	2622	4095	5707
Discontinuous dense urban fabric	969	1401	1808	2329	3159
Discontinuous medium density urban fabric	1021	1286	1446	1888	2617
Discontinuous low density urban fabric	502	895	1175	2331	3221
Industrial, commercial, and transport units	473	685	991	1245	1717
Arable land and permanent crops	2009	2119	2409	2009	2776
Forests, scrubs, and other natural areas	1449	1463	1559	1568	1974
Other (open spaces, bare land, mines, inland water)	453	460	475	525	574
Total	8674	10,630	12,485	15,990	21,745
	Validation				
Total	3637	4319	5419	6919	9399

RF is known to be efficient with large data handling, to provide a reduced likelihood of over-fitting and that it is suitable for multi-source inputs [32,43,50]. The classification models involved 20 variables in total: besides the six reflective Landsat bands (bands 1–5 and 7 for Landsat 5 TM and Landsat 7 ETM+, bands 2–7 for Landsat 8 OLI), the thermal band was also used as it has been proven to help in the classification process [52]. In addition, the first layer produced by a principal component analysis (PCA) separately for the three visible bands (1, 2, and 3) and the infrared bands (5 and 7), was also incorporated, as it has been shown to increase classification accuracy [32,53]. The Normalized Difference Built-up Index (NDBI) [54] and the Enhanced Built-up and Bareness Index (EBBI) [55] were also incorporated to enhance the discrimination of the urban LUC types. The Enhanced Vegetation Index (EVI) [56], the Normalized Difference Moisture Index (NDMI) [57], the Normalized Difference Bareness Index (NDBaI) [54], and the Normalized Differential Vegetation Index (NDVI) [58] were also included because of their capacity to separate vegetation from bare features during the classification process. The three widely used Tasseled Cap (TC) transformations, namely, the Soil Brightness Index (SBI), the Green Vegetation Index (GVI), and the Moisture Content of Soil/Vegetation (Wetness), were also included in the analysis [59]. Finally, auxiliary relief-related variables of elevation and slope were acquired from the Global Land Survey Digital Elevation Model (GLSDEM) [60] and included in the modeling.

2.5. RF Classification and Accuracy Assessment

All images were classified into eight LUC categories, implementing the RF classification algorithm through the RandomForest package available in R [61]. To set up the models, RF requires two primary parameters to be specified: the number of predictor variables randomly sampled at each decision tree split and the number of classification trees to be built. Four predictor variables were chosen for each tree split, which is equal to the square root of the total number of predictor variables and 500 trees for each run. To deal with the so called 'salt-n-pepper' effect of the resulting maps, all isolated patches (defined as areas less than 0.1 ha), were removed by replacing their category value with the mode of their neighborhood pixels, defined by a 3 × 3 window [32,43,50]. Results were plotted against the 30% of the initial samples and the error matrix produced using a cross-tabulation approach [32,43].

2.6. Change Detection

In order to map and quantify the spatiotemporal patterns of LUC changes, we applied change detection techniques in the form of post-classification comparisons. Specifically, cross-classification and cross-tabulation [43,52] were employed in order to quantify LUC changes. This step was deemed important to highlight the changes that occurred during the study period and to temporarily allocate these changes, enabling possible associations with significant events that occurred in the area (e.g.,

new International Airport, Athens 2004 Olympics) and with different phases of economic realities and performance.

3. Results

Overall accuracies were high and ranged from 90.5% to 93.5%. (Table 3). Regarding the disagreements, confusion between certain classes can be observed between "discontinuous medium density urban fabric" and "discontinuous low density urban fabric", as well as between "discontinuous low density urban fabric" and "arable land and permanent crops". These classes are often spectrally and visually similar, resulting in confusion between the spectral signatures.

The LUC maps were tabulated in order to observe the fluctuations in LUC categories throughout the study period. Results revealed that Attica experienced three distinct and uneven periods of LUC change. Figure 2 provides a quantification of the periodic changes that occurred in Attica over the last 25 years. The most significant changes were the urban and industrial expansion, which started to be evident in 1999 and peaked in 2010. In particular, the discontinuous low density urban fabric started to increase rapidly in 2003, reaching 7% (from 2.5% in 1991). This trend continued until 2016, reaching 12%. The continuous as well as the discontinuous dense urban fabric almost doubled throughout the study period, reaching 5.5% and 4.8% in 2016, while in 1991 they were 2.6% and 2.3%, respectively. It is worth noting that, after 2010, the development trends remained positive but started to decline as a consequence of the dramatic decrease in internal and external investment and the collapse in the housing demand and supply equilibrium. All of the artificial areas development took place at the expense of agricultural areas, which accounted for about 40% in 1991 and declined to 23.5% in 2016. The forests, scrubs, and other natural areas category remained relatively stable, decreasing only by 3% in 25 years.

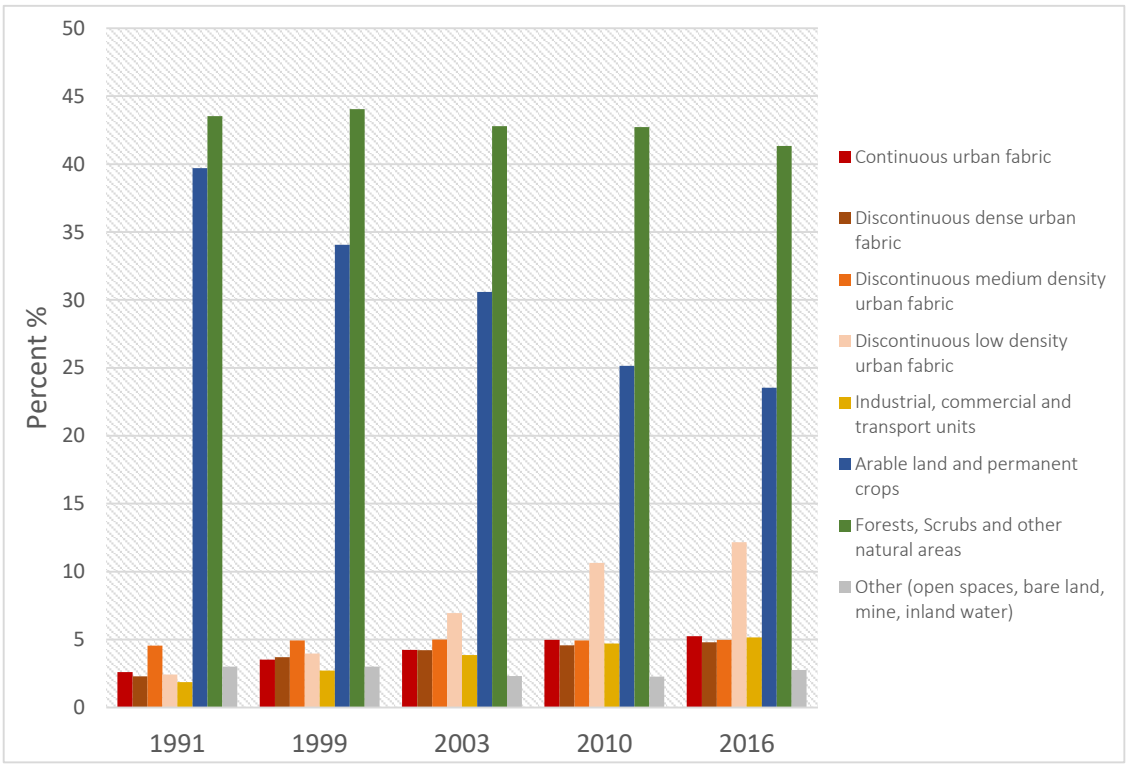

Figure 2. Summary of statistics based on the five classified maps and percentage of LUC categories.

Table 3. Error matrix—resulting map per year against reference samples. U.A: User's Accuracy; P.A: Producer's Accuracy; O.A: Overall Accuracy. 1: Continuous urban fabric. 2: Discontinuous dense urban fabric. 3: Discontinuous medium density urban fabric. 4: Discontinuous low density urban fabric. 5: Industrial, commercial, and transport units. 6: Arable land and permanent crops. 7: Forests, scrubs, and other natural areas. 8: Other (open spaces, bare land, mines, inland water).

		1991									**1999**								
		Result									***Result***								
		1	**2**	**3**	**4**	**5**	**6**	**7**	**8**	**P.A**	**1**	**2**	**3**	**4**	**5**	**6**	**7**	**8**	**P.A**
Reference	1	681	11	3		9				97%	1012	28	6		8				96%
	2	14	631	28		12	2	2	2	91%	58	1174	22		18	2	6	14	91%
	3	31	51	1710	58	4	6	6	4	91%	32	67	1833	15	15	6	3	11	92%
	4	8	20	104	1288	12	20	10	8	88%		28	90	1426	36	24	12	4	88%
	5		10	15	10	515	15	5	10	89%	25	20	15	5	859	15		10	91%
	6	12	13	40	148	24	6576	168	28	94%	6	46	48	196	26	4946	120	26	91%
	7		8	6	42	11	109	2337	11	93%		21	63	22	16	188	2427	19	88%
	8			1	7	10	16	11	258	85%			10	24	14	28	14	456	84%
	U.A	91%	85%	90%	83%	86%	98%	92%	80%		89%	85%	88%	84%	87%	95%	94%	84%	
	O.A	92.2%									90.5%								
		2003									**2010**								
		Result									***Result***								
		1	**2**	**3**	**4**	**5**	**6**	**7**	**8**	**P.A**	**1**	**2**	**3**	**4**	**5**	**6**	**7**	**8**	**P.A**
Reference	1	1323	42	10		19			1	95%	1838	51	21		14		1		95%
	2	56	1658	52	4	20	8	6	4	92%	72	2241	42	10	36	4	8	12	92%
	3	30	35	2276	30	38	3	12	16	93%	21	46	2299	63	31	15	21	9	92%
	4		48	86	2682	56	64	24	12	90%		48	91	3246	76	42	40	10	91%
	5	25	20	15	20	1165	30	10	10	90%	33	20	40	21	1798	25		7	92%
	6		32	46	228	38	4128	60	16	91%		6	18	162	54	4091	64	12	93%
	7		7	21	61	21	224	2860	24	89%		14		48	28	207	3528	14	92%
	8			8	6	14	20	19	443	87%		8		16	11	14	20	490	88%
	U.A	92%	90%	91%	88%	85%	92%	96%	84%		94%	92%	92%	91%	88%	93%	96%	88%	
	O.A	90.7%									92.3%								

Table 3. *Cont.*

		2016								
		Result								
		1	**2**	**3**	**4**	**5**	**6**	**7**	**8**	**P.A**
Reference	1	2683	59	19		24		2	2	96%
	2	80	3252	76	18	42	22	10	8	93%
	3	24	61	2964	101	35	17	36	20	91%
	4	4	32	92	5446	78	112	44	1	94%
	5	55	30	30	30	2325	105		17	90%
	6		6	12	36	30	4866	66	26	97%
	7		14		35	28	182	4823	22	94%
	8				16	16	34	24	616	87%
	U.A	94%	94%	93%	96%	90%	91%	96%	87%	
	O.A	93.5%								

To highlight the observed trajectories of the most prominent changes, a suite of maps portraying the major LUC change was created. Figure 3 depicts the urban expansion as well as the increase in density that occurred during the last 25 years in Attica. Urban sprawl is obvious mostly in the northern and eastern parts of Attica, less so in the west. The majority of sprawl occurred along the waterfront, especially in Messoghia, Marathonas, north Attica, and southeast of Athens. The affluent northern suburbs of Athens also experienced a certain degree of urban growth, but the dominant type of change in this area was the infill that consequently led to a significant increase in density. Also notable is the pattern of uneven development between the three different periods.

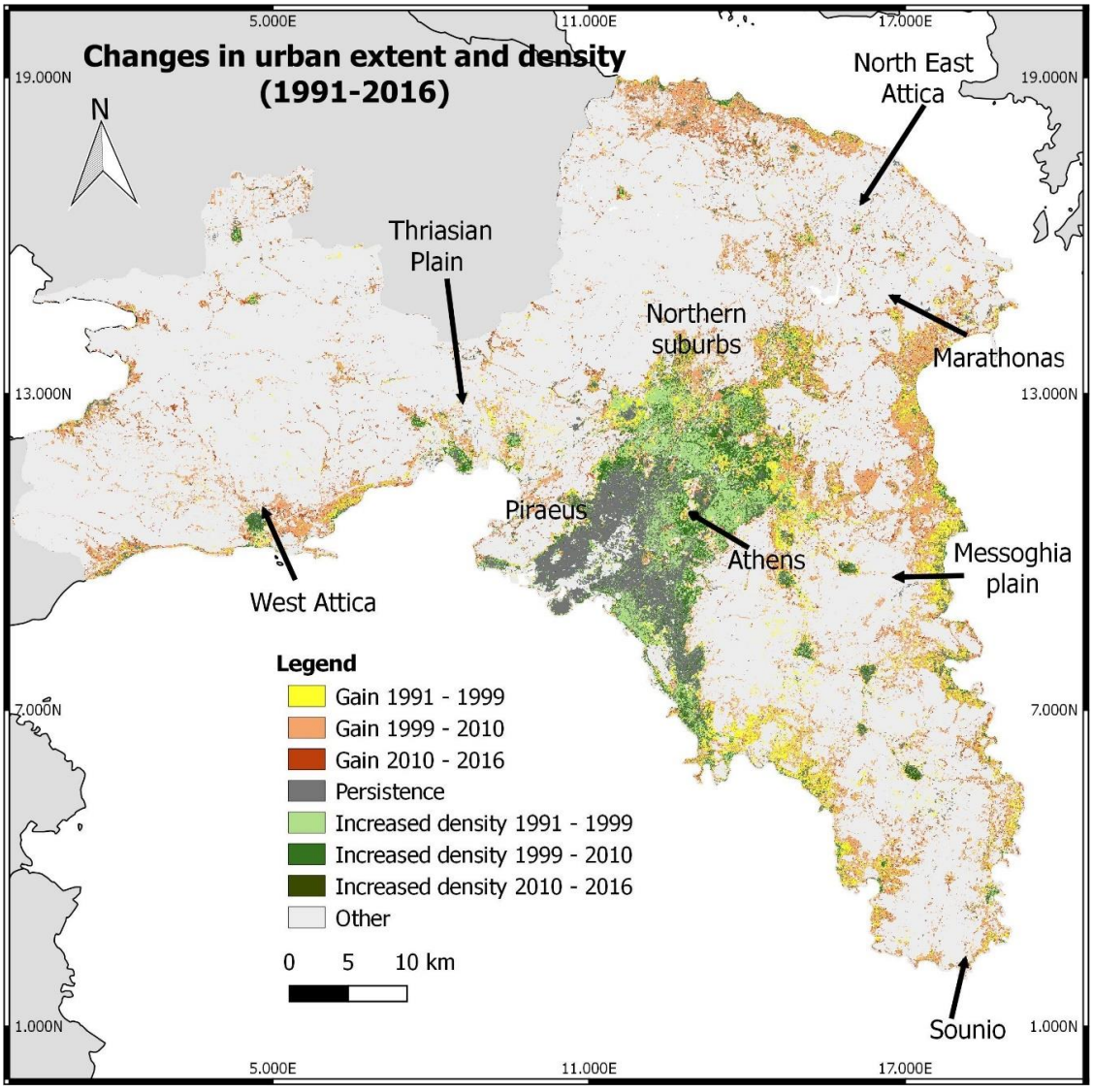

Figure 3. Urban trajectories observed between 1991 and 2016 (includes all urban fabric categories).

Figure 4 depicts the expansion of industrial, commercial, and transport units that occurred over the last 25 years in Attica. The Thriassian plain, located in the west of Athens, as well as Messoghia plain located to the east experienced the largest amount of this type of LUC change.

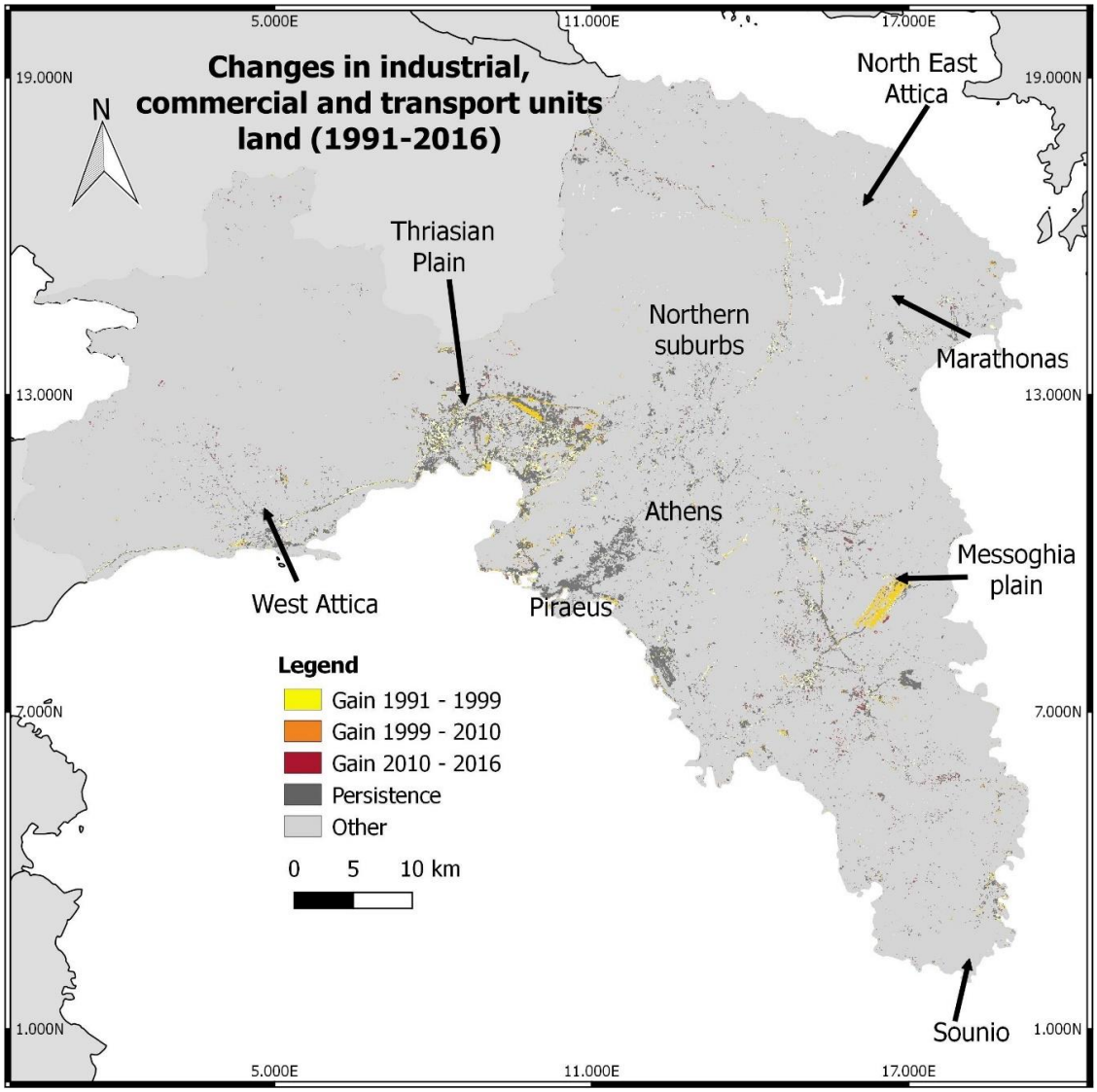

Figure 4. Industrial expansion observed between 1991 and 2016.

The urban and industrial expansion that occurred over the last 25 years in Attica has mostly taken place at the expense of agricultural land. Figure 5 depicts the aggregated loss of agricultural land over the study period. As can be seen, almost all surrounding land of the greater Athens metropolitan area experienced agricultural land loss. As in the case of the urban and industrial expansion (Figures 3 and 4), the agricultural land loss is more evident in the Thriassian plain, west Attica, north Attica, Marathonas, the Messoghia plain, and southeast of Athens. The vast majority of this loss occurred during the period of 1991–2010. Figure 6 depicts the LUC changes related to the forests, scrubs, and other natural areas, which experienced a relatively slight decrease.

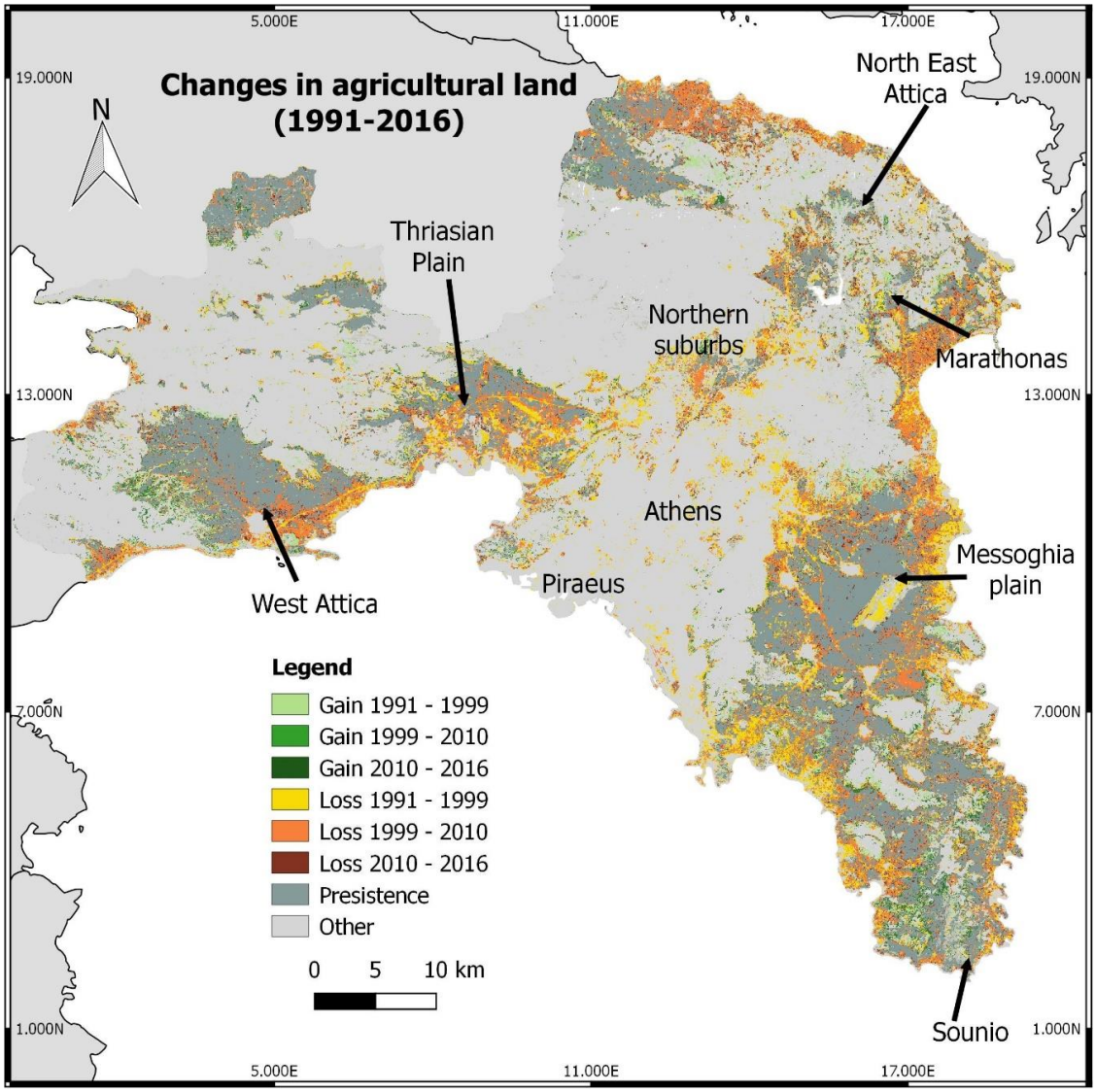

Figure 5. Changes in agricultural land observed between 1991 and 2016.

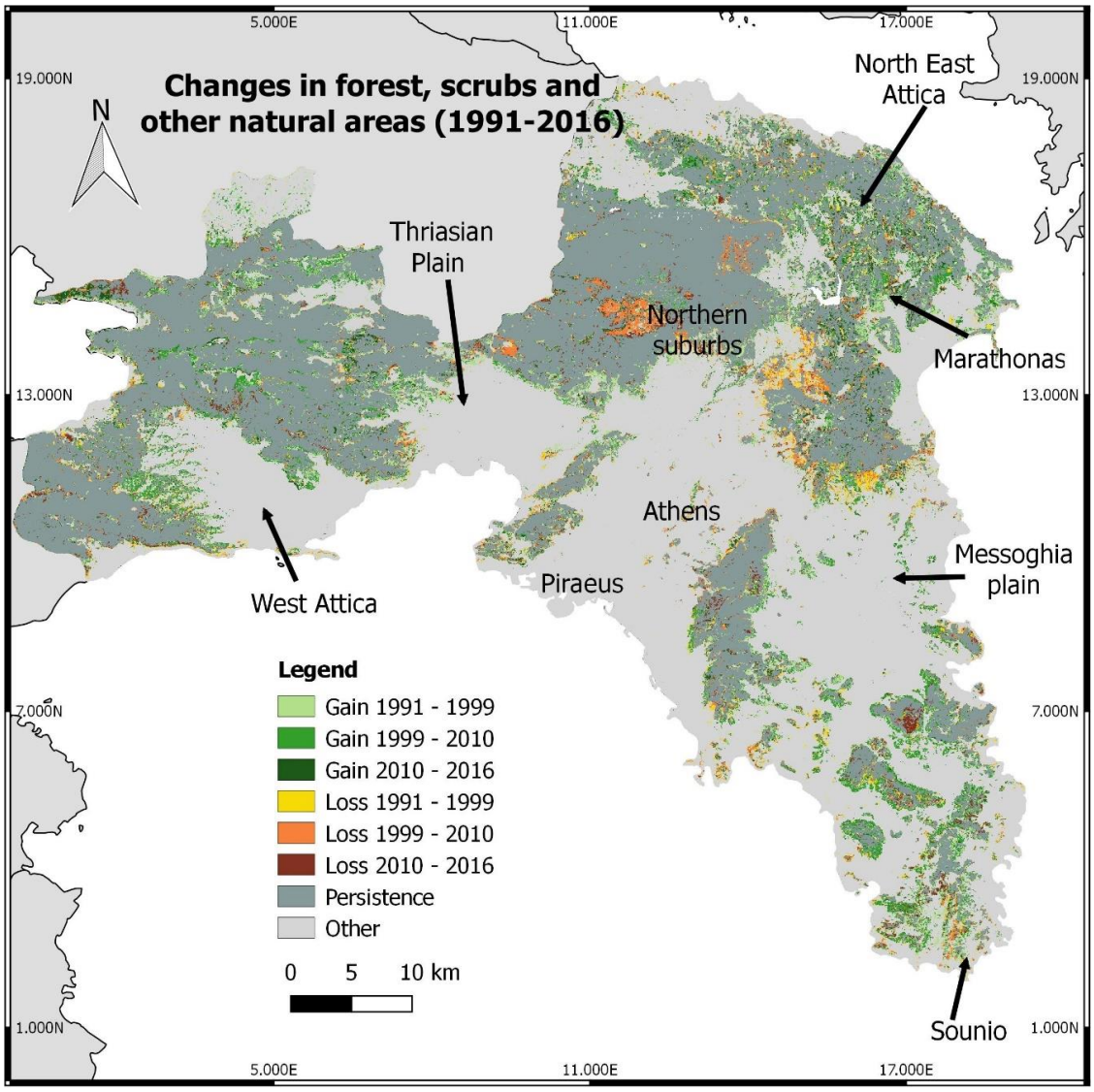

Figure 6. Changes in forests and natural areas observed between 1991 and 2016.

4. Discussion

LUC Change in Attica

The majority of LUC changes took place during the 1999–2010 period, while in the following years (until 2016) urban growth in the area was notably curtailed. Regarding urban form, the types of sprawl noted in the region are varied, including leap-frog development, suburban growth, as well as strip and scattered development, a fact that is attributed to the loose spatial planning framework, facilitating unregulated urban expansion. Land use zoning schemes in Attica, for instance, were instituted in a scattered fashion in the 1996–2003 period, dividing the area into sections and avoiding a coherent approach. Still, as one in four local authorities lacked a detailed land use plan, the belated and haphazard introduction of zoning did not affect developments on the ground. Zoning did not inform the (missing) municipal land use plans. Construction rights, therefore, were only limited by the size of the plot to be developed [62]. The impact of unregulated urban growth was particularly apparent in the Thriassian and Messoghia plains due to the tendency of middle-class Athenians to move to areas with lower density [63,64].

During the 1991–1999 period, the Thriassian plain in the northwest faced a notable industrial expansion, while in the following years (1999–2010) the construction of the new international airport in Messoghia dominated developments eastwards. These two areas attracted urban growth due to two main advantages. First, the establishment of new transportation networks in the area during the 1990s, the Athens ring road and the suburban railway, enhanced their connectivity with the city of Athens, the region's main economic center. Additionally, the availability of low-cost and morphologically suitable land facilitated construction activities. These two areas, however, have different attributes. The Thriassian plain is mainly occupied by industrial facilities such as oil refineries, steel mills, military bases, and transshipment hubs. The Messoghia plain, on the other hand, is occupied by residential and commercial areas, as well as by large physical infrastructure facilities, such as Olympics-related venues.

Land use change from agricultural to urban uses occurred primarily in the 1991–2010 period. Urban development in a specific location is associated in the literature with an increase in the market value of nearby land, a trait which explains why residential, industrial, and commercial uses tend to dominate over less profitable land in the bid for space [65]. As agricultural land was available at a relatively lower cost than other land uses, land speculation was encouraged and land use change was facilitated by the weak presence of spatial planning controls. Changes took place in the urban periphery, especially in areas adjacent to existing urban agglomerations. Losses of agricultural land can be seen in many areas in the region, including the northern suburbs of Athens, the periphery of Hymettus mountain, and Cape Sounio. In these parts, land use change is also associated with deliberately caused wildfires, directly related to land speculation [66].

The results of this paper highlight the relevance of economic circumstances in shaping LUC change [40,41]. In particular, as demonstrated by the LUC change detection, the built-up expansion rates in Attica are highly correlated with economic development fluctuations. In the 1999–2009 period, high economic development rates accompanied by significant investments in physical infrastructure networks expedited the expansion of built-up land in the region. Conversely, during economic austerity and recession (2010–2016), investments in real estate and transactions in the respective market were notably held back. It should be stressed though that LUC changes in the region and, in particular, the type and intensity of urban expansion, was also influenced by the underdeveloped traits of the land use planning apparatus. Reflecting on the above can serve as a basis to project the observed trends to future decades, sketching distinct and alternative LUC change scenarios for Attica [43,67].

The RF algorithm was proven to be robust in the face of the complex task that involved the accomplishment of a very high thematic resolution to disaggregate the urban-related LUC categories and their temporal trajectories. Additionally, the algorithm successfully handled the large amount of input data, both in the form of the training samples as well as the various predictor variables that were incorporated in the models. The discrimination of LUC categories according to their density and continuity was an important step, because it provided unique insights into the LUC system. If this step had not been undertaken and a more conventional nomenclature of LUC classes had been adopted, the majority of changes would have been ignored, e.g., the changes in density observed in the northern suburbs of Athens, where the extent remained relatively constant while the density increased dramatically.

EO coupled with geoinformatics is a sound approach for accurately and cost-effectively extracting spatiotemporal information related to LUC. The open-access Landsat archive is particularly suitable for detecting large-scale historical LUC changes, since it constitutes the longest record of the Earth's surface. The only compromise related to the use of Landsat data in urban LUC studies is the spatial resolution of 30-m pixels. Satellite sensors record the emitted energy of objects and each satellite image is therefore a file of spectral signatures, translated by users as information about the objects. Each pixel represents the spectral characteristics of all objects found in a 900-m^2 area. Apparently, this translates to information loss and could be crucial to such urban studies. However, the ratio involving price, spatial resolution, and size is almost inversely proportional and for this reason it must be taken into account that the level of detail, the available budget, and the purpose of study are complementary.

The temporal resolution was also an important aspect of the analysis. The inclusion of five distinct epochs in the analysis provided clearer insights into the spatiotemporal dynamics of LUC and played a key role in the identification of three distinct periods of uneven development. Using fewer time steps, as is the case in numerous approaches, would have impeded this. The use of more steps would have increased computational times significantly without any clear benefits, as the propagation of errors would have been even greater [68].

The semi-automated sampling techniques demonstrated in this paper were proven to offer a sound approach for overcoming the need for exhaustive methodologies in order to train classification algorithms. Arduous training methods tend to prevent many researchers from carrying out LUC mapping exercises in high temporal resolution. Given that changes usually occur in a small fraction of land and especially at borders between LUC types, extracting information as training from already available datasets, utilizing unchanged areas as a training source, was considered a reasonable option. In this way, the potential error that would likely propagate, thus undermining the whole process, would be due to the incompatibility between datasets and scales. To overcome this, we relocated and/or removed training points away from the boundaries between adjacent categories. However, this strategy entails a certain degree of bias towards more homogenous areas.

Regarding the RF classification process, the amount of training samples can be crucial for producing accurate classifications. The modeling also benefits from the inclusion of a number of samples that is proportional to the area covered by each LUC category. It was found that the classification accuracy increases with the size of the training data but the distribution of the samples, with a good range of intra-class variability, is of equal importance [69].

5. Conclusions

This paper presented a methodological framework for the accurate detection of LUC changes that occurred in the Attica region of Greece over a 25-year period. We demonstrated an operational, cost-effective, and fully transferable approach that is able to map LUC in a high thematic resolution, considering not only the prominent changes between major LUC categories, but also changes in density and continuity. The use of high thematic resolution was able to reveal patterns and aspects of LUC change that would have been ignored if a more conventional categorization of LUC types had been adopted. The presented approach comes with a high degree of automation in the process, is fully transferable, and can act as a baseline for the continuous monitoring of LUC using medium-scale EO data.

Author Contributions: D.G. and S.K. conceived of and designed the experiments. D.G. performed the experiments, interpreted the results, and wrote the manuscript. E.S., I.C., and S.K. proofread and contributed to the writing and revising of the manuscript.

Funding: This research received no external funding.

Acknowledgments: The authors wish to thank the anonymous reviewers and the Assigned Editor for their constructive criticism and suggestions on an earlier version of this manuscript.

Conflicts of Interest: The authors declare no conflict of interest.

References

1. Sagan, C.; Toon, O.B.; Pollack, J.B. Anthropogenic albedo changes and the Earth's climate. *Science* **1979**, *206*, 1363–1368. [CrossRef] [PubMed]
2. Meyer, W.B.; Turner, B.L., II. Land-use/land-cover change: Challenges for geographers. *GeoJournal* **1996**, *39*, 237–240. [CrossRef]
3. Vitousek, P.M.; Mooney, H.A.; Lubchenco, J.; Melillo, J.M. Human domination of Earth's ecosystems. *Science* **1997**, *277*, 494–499. [CrossRef]
4. Feddema, J.J.; Oleson, K.W.; Bonan, G.B.; Mearns, L.O.; Buja, L.E.; Meehl, G.A.; Washington, W.M. The Importance of Land-Cover Change in Simulating Future Climates. *Science* **2005**, *310*, 1674–1678. [CrossRef] [PubMed]

5. Gibbs, H.K.; Salmon, J.M. Mapping the world's degraded lands. *Appl. Geogr.* **2015**, *57*, 12–21. [CrossRef]
6. Turner, B.L., II. Local faces, global flows: The role of land use and land cover in global environmental change. *Land Degrad. Rehabil.* **1994**, *5*, 71–78. [CrossRef]
7. Coppin, P.; Jonckheere, I.; Nackaerts, K.; Muys, B. Digital change detection methods in ecosystem monitoring: A review. *Int. J. Remote Sens.* **2004**, *25*, 1565–1596. [CrossRef]
8. Rozenstein, O.; Karnieli, A. Comparison of methods for land-use classification incorporating remote sensing and GIS inputs. *Appl. Geogr.* **2011**, *31*, 533–544. [CrossRef]
9. Belward, A.S.; Skøien, J.O. Who launched what, when and why; trends in global land-cover observation capacity from civilian earth observation. *ISPRS J. Photogramm.* **2014**, *103*, 115–128. [CrossRef]
10. Hansen, M.C.; Potapov, P.V.; Moore, R.; Hancher, M.; Turubanova, S.A.; Tyukavina, A.; Thau, D.; Stehman, S.V.; Goetz, S.J.; Loveland, T.R.; et al. High-Resolution Global Maps of 21st-Century Forest Cover Change. *Science* **2013**, *342*, 850–853. [CrossRef] [PubMed]
11. Schneider, A.; Friedl, M.A.; Potere, D. A new map of global urban extent from MODIS satellite data. *Environ. Res. Lett.* **2009**, *4*, 044003. [CrossRef]
12. Zhu, Z.; Woodcock, C.E. Continuous change detection and classification of land cover using all available Landsat data. *Remote Sens. Environ.* **2013**, *144*, 152–171. [CrossRef]
13. Hansen, M.C.; Loveland, T.R. A review of large area monitoring of land cover change using Landsat data. *Remote Sens. Environ.* **2012**, *122*, 66–74.
14. Wulder, M.A.; Masek, J.G.; Cohen, W.B.; Loveland, T.R.; Woodcock, C.E. Opening the archive: How free data has enabled the science and monitoring promise of Landsat. *Remote Sens. Environ.* **2012**, *122*, 2–10. [CrossRef]
15. Giri, C.; Pengra, B.; Long, J.; Loveland, T.R. Next generation of global land cover characterization, mapping, and monitoring. *Int. J. Appl. Earth Obs.* **2013**, *25*, 30–37. [CrossRef]
16. Herold, M.; Mayaux, P.; Woodcock, C.E.; Baccini, A.; Schmullius, C. Some challenges in global land cover mapping: An assessment of agreement and accuracy in existing 1 km datasets. *Remote Sens. Environ.* **2008**, *112*, 2538–2556. [CrossRef]
17. Conway, T.M. The impact of class resolution in land use change models. *Comput. Environ. Urban* **2009**, *33*, 269–277. [CrossRef]
18. Pontius, R.G., Jr.; Malizia, N.R. Effect of category aggregation on map comparison. In *GIScience 2004*; Engenhofer, M.J., Freska, C., Miller, H.J., Eds.; Springer: New York, NY, USA, 2004; pp. 251–268.
19. Buyantuyev, A.; Wu, J. Effects of thematic resolution on landscape pattern analysis. *Landsc. Ecol.* **2007**, *22*, 7–13. [CrossRef]
20. Liang, Y.; He, H.; Fraser, J.S.; Wu, Z.W. Thematic and Spatial Resolutions Affect Model-Based Predictions of Tree Species Distribution. *PLoS ONE* **2013**, *8*, e67889. [CrossRef] [PubMed]
21. Zhou, W.; Qian, Y.; Li, X.; Li, W.; Han, L. Relationships between land cover and the surface urban heat island: Seasonal variability and effects of spatial and thematic resolution of land cover data on predicting land surface temperatures. *Landsc. Ecol.* **2014**, *29*, 153–167. [CrossRef]
22. Bailey, D.; Herzog, F.; Augenstein, I.; Aviron, S.; Billeter, R.; Szerencsits, E.; Baudry, J. Thematic resolution matters: Indicators of landscape pattern for European agro-ecosystems. *Ecol. Indic.* **2007**, *7*, 692–709. [CrossRef]
23. Símová, P.; Gdulová, K. Landscape indices behavior: A review of scale effects. *Appl. Geogr.* **2012**, *34*, 385–394. [CrossRef]
24. Potere, D.; Schneider, A.; Angel, S.; Civco, D.L. Mapping urban areas on a global scale: Which of the eight maps now available is more accurate? *Int. J. Remote Sens.* **2009**, *30*, 6531–6558. [CrossRef]
25. Bossard, M.; Feranec, J.; Otahel, J. *CORINE Land Cover Technical Guide—Addendum 2000 (Report No. 40)*; European Environment Agency: Copenhagen, Denmark, 2000.
26. Chen, J.; Chen, J.; Liao, A.; Cao, X.; Chen, L.; Chen, X.; He, C.; Han, G.; Peng, S.; Lu, M.; et al. Global land cover mapping at 30 m resolution: A POK-based operational approach. *ISPRS J. Photogramm.* **2015**, *103*, 7–27. [CrossRef]
27. Chen, X.; Chen, J.; Shi, Y.; Yamaguchi, Y. An automated approach for updating land cover maps based on integrated change detection and classification methods. *ISPRS J. Photogramm.* **2012**, *71*, 86–95. [CrossRef]
28. Comber, A.J.; Law, A.N.R.; Lishman, J.R. Application of knowledge for automated land cover change monitoring. *Int. J. Remote Sens.* **2004**, *25*, 3177–3192. [CrossRef]

29. Huth, J.; Kuenzer, C.; Wehrmann, T.; Gebhardt, S.; Quoc Tuan, V.; Dech, S. Land Cover and Land Use Classification with TWOPAC: Towards Automated Processing for Pixel- and Object-Based Image Classification. *Remote Sens.* **2012**, *4*, 2530–2553. [CrossRef]
30. Radoux, J.; Lamarche, C.; Van Bogaert, E.; Bontemps, S.; Brockmann, C.; Defourny, P. Automated Training Sample Extraction for Global Land Cover Mapping. *Remote Sens.* **2014**, *6*, 3965–3987. [CrossRef]
31. Yuan, H.; Van Der Wiele, C.F.; Khorram, S. An Automated Artificial Neural Network System for Land Use/Land Cover Classification from Landsat TM Imagery. *Remote Sens.* **2009**, *1*, 243–265. [CrossRef]
32. Gounaridis, D.; Apostolou, A.; Koukoulas, S. Land Cover of Greece, 2010: A semi-automated classification using Random Forests. *J. Maps* **2016**, *12*, 1055–1062. [CrossRef]
33. Jiang, D.; Huang, Y.; Zhuang, D.; Zhu, Y.; Xu, X.; Ren, H. A Simple Semi-Automatic Approach for Land Cover Classification from Multispectral Remote Sensing Imagery. *PLoS ONE* **2012**, *7*, e45889. [CrossRef] [PubMed]
34. Xian, G.; Collin, H.; Fry, J. Updating the 2001 National Land Cover Database land cover classification to 2006 by using Landsat imagery change detection methods. *Remote Sens. Environ.* **2009**, *113*, 1133–1147. [CrossRef]
35. Klein, I.; Gessner, U.; Kuenzer, C. Regional land cover mapping and change detection in Central Asia using MODIS time-series. *Appl. Geogr.* **2012**, *35*, 219–234. [CrossRef]
36. Mantouvalou, M.; Mavridou, M.; Vaiou, D. Processes of social integration and urban development in Greece: Southern challenges to European unification. *Eur. Plan. Stud.* **1995**, *3*, 189–204. [CrossRef]
37. Leontidou, L.; Afouxenidis, A.; Kourliouros, E.; Marmaras, E. *Infrastructure-Related Urban Sprawl: Mega-Events and Hybrid Peri-Urban Landscapes in Southern Europe, in Urban Sprawl in Europe: Landscapes, Land-Use Change & Policy*; Couch, C., Leontidou, L., Petschel-Held, G., Eds.; Blackwell Publishing Ltd.: Oxford, UK, 2007.
38. Arapoglou, V.P.; Sayas, J. New facets of urban segregation in southern Europe. *Eur. Urban Reg. Stud.* **2009**, *16*, 345–362. [CrossRef]
39. Pagonis, A. *The Evolution of Metropolitan Planning Policy in Athens over the Last Three Decades: Linking Shifts in the Planning Discourse with Institutional Changes and Spatial Transformation. Changing Cities: Spatial, Morphological, Formal and Socioeconomic Dimensions*; University of Thessaly: Skiathos, Greece, 2013.
40. Chorianopoulos, I.; Pagonis, A.; Koukoulas, S.; Drymoniti, S. Planning, competitiveness and sprawl in the Mediterranean city: The case of Athens. *Cities* **2010**, *27*, 249–259. [CrossRef]
41. Chorianopoulos, I.; Tsilimigkas, G.; Koukoulas, S.; Balatsos, T. The shift to competitiveness and a new phase of sprawl in the Mediterranean city: Enterprises guiding growth in Messoghia—Athens. *Cities* **2014**, *39*, 133–143. [CrossRef]
42. Bank of Greece. *Summary of the Annual Report (2015)*; Bank of Greece: Athens, Greece, 2016.
43. Gounaridis, D.; Chorianopoulos, I.; Koukoulas, S. Exploring prospective urban growth trends under different economic outlooks and land-use planning scenarios: The case of Athens. *Appl. Geogr.* **2018**, *90*, 134–144. [CrossRef]
44. Municipality of Athens. *Study on Market Trends and Development*; Centre for Entrepreneurial Support: Athens, Greece, 2014.
45. Chavez, P.S., Jr. An improved dark-object subtraction technique for atmospheric scattering correction of multi-spectral data. *Remote Sens. Environ.* **1988**, *24*, 459–479. [CrossRef]
46. Vermote, E.; Tanré, D.; Deuzé, J.L.; Herman, M.; Morcrette, J.-J. Second Simulation of the Satellite Signal in the Solar Spectrum, 6S: an overview. *IEEE Trans. Geosci. Remote Sens.* **1997**, *35*, 675–686. [CrossRef]
47. Civco, D.L. Topographic normalization of Landsat thematic mapper digital imagery. *Photogramm. Eng. Remote Sens.* **1989**, *55*, 1303–1309.
48. Teillet, P.M.; Guindon, B.; Goodenough, D.G. On the slope-aspect correction of multispectral scanner data. *Can. J. Remote Sens.* **1982**, *8*, 84–106. [CrossRef]
49. European Commission. *Urban Atlas—Delivery of Land Use/Cover Maps of Major European Agglomerations*; Final Report V 2.0; European Commission: Brussels, Belgium, 2011.
50. Gounaridis, D.; Koukoulas, S. Urban land cover thematic disaggregation, employing datasets from multiple sources and RandomForests modelling. *Int. J. Appl. Earth Obs.* **2016**, *51*, 1–10. [CrossRef]
51. Kim, D.-H.; Sexton, J.O.; Noojipady, P.; Huang, C.; Anand, A.; Channan, S.; Feng, M.; Townshend, J.R. Global, Landsat-based forest-cover change from 1990 to 2000. *Remote Sens. Environ.* **2014**, *155*, 178–193. [CrossRef]

52. Rodriguez-Galiano, V.F.; Chica-Olmo, M. Land cover change analysis of a Mediterranean area in Spain using different sources of data: Multi-seasonal landsat images, land surface temperature, digital terrain models and texture. *Appl. Geogr.* **2012**, *35*, 208–218. [CrossRef]
53. Gounaridis, D.; Zaimes, N.G.; Koukoulas, S. Quantifying spatio-temporal patterns of forest fragmentation in Hymettus Mountain, Greece. *Comput. Environ. Urban* **2014**, *46*, 35–44. [CrossRef]
54. Zha, Y.; Gao, J.; Ni, S. Use of normalized difference built-up index in automatically mapping urban areas from TM imagery. *Int. J. Remote Sens.* **2003**, *24*, 583–594. [CrossRef]
55. As-Syakur, A.R.; Adnyana, I.; Arthana, I.W.; Nuarsa, I.W. Enhanced built-up and bareness index (EBBI) for mapping built-up and bare land in an urban area. *Remote Sens.* **2012**, *4*, 2957–2970. [CrossRef]
56. Huete, A.; Didan, K.; Miura, T.; Rodriguez, E.P.; Gao, X.; Ferreira, L.G. Overview of the radiometric and biophysical performance of the MODIS vegetation indices. *Remote Sens. Environ.* **2002**, *83*, 195–213. [CrossRef]
57. Cibula, W.G.; Zetka, E.F.; Rickman, D.L. Response of thematic mapper bands to plant water stress. *Int. J. Remote Sens.* **1992**, *13*, 1869–1880. [CrossRef]
58. Tucker, C.J. Red and photographic infrared linear combinations for monitoring vegetation. *Remote Sens. Environ.* **1979**, *8*, 127–150. [CrossRef]
59. Crist, E.P. A TM tasseled cap equivalent transformation for reflectance factor data. *Remote Sens. Environ.* **1985**, *17*, 301–306. [CrossRef]
60. USGS. *GLSDEM, 90 m Scene GLSDEM_p123r024_utmz13*; Global Land Cover Facility, University of Maryland: College Park, MD, USA, 2008.
61. Liaw, A.; Wiener, M. Classification and regression by RandomForest. *R News* **2002**, *2*, 18–22.
62. Tsilimigkas, G.; Stathakis, D.; Pafi, M. Evaluating the land use patterns of medium-sized Hellenic cities. *Urban Res. Pract.* **2015**, *9*, 181–203. [CrossRef]
63. Morelli, V.G.; Salvati, L. *Ad Hoc Urban Sprawl in the Mediterranean City: Dispersing a Compact Tradition?* Nuova Cultura: Rome, Italy, 2010.
64. Lagarias, A.; Sayas, J. Comparing Peri-Urban Patterns of Greek Cities Using Spatial Metrics to Measure Urban Sprawl. Conference Proceedings: Cities and Regions in a Changing Europe: Challenges and Prospects, 5–7 July, Panteion University, Athens, Greece. 2017. Available online: http://asrdlf2017.com/asrdlf2017_com/envoitextefinal/auteur/textedef/219.pdf (accessed on 29 June 2018).
65. Guy, S.; Henneberry, J. *Development and Developers: Perspectives on Property*; Blackwell: Oxford, UK, 2008.
66. Tsilimigkas, G.; Kizos, T.; Gourgiotis, A. Unregulated urban sprawl and spatial distribution of fire events: Evidence from Greece. *Environ. Hazards* **2018**. [CrossRef]
67. Gounaridis, D.; Chorianopoulos, I.; Symeonakis, E.; Koukoulas, S. A Random Forest-Cellular Automata modelling approach to explore future land use/cover change in Attica (Greece), under different socio-economic realities and scales. *Sci. Total Environ.* **2018**, submitted.
68. Symeonakis, E.; Caccetta, P.; Koukoulas, S.; Furby, S.; Karathanasis, N. Multi-temporal land cover classification and change analysis with Conditional Probability Networks: The case of Lesvos Island (Greece). *Int. J. Remote Sens.* **2012**, *33*, 4075–4093. [CrossRef]
69. Colditz, R.R. An Evaluation of Different Training Sample Allocation Schemes for Discrete and Continuous Land Cover Classification Using Decision Tree-Based Algorithms. *Remote Sens.* **2015**, *7*, 9655–9681. [CrossRef]